

ADA129493



AD

AMMRC TR 82-8

EROSIVE EFFECTS OF VARIOUS PURE AND  
COMBUSTION GENERATED GASES ON METALS

February 1982

BARRIE S. H. ROYCE  
Princeton University  
Department of Mechanical and Aerospace Engineering  
Princeton, New Jersey 08544

FINAL REPORT

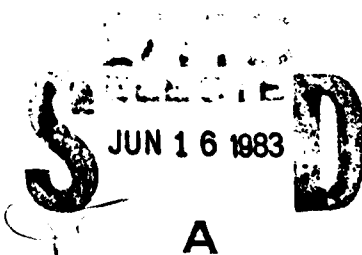
Contract No. DAAG46-80-C-0012

Approved for public release; distribution unlimited.

DTIC FILE COPY

Prepared for

ARMY MATERIALS AND MECHANICS RESEARCH CENTER  
Watertown, Massachusetts 02172



83 06 15 043

The findings in this report are not to be construed as an official Department of the Army position, unless so designated by other authorized documents.

Mention of any trade names or manufacturers in this report shall not be construed as advertising nor as an official indorsement or approval of such products or companies by the United States Government.

**DISPOSITION INSTRUCTIONS**

**Destroy this report when it is no longer needed.  
Do not return it to the originator.**





THE EROSION EFFECTS OF VARIOUS PURE AND COMBUSTION-  
GENERATED GASES ON METALS

I. INTRODUCTION

The experimental studies to be reported in this document represent the closing phase of a metal erosion program that has involved the use of both a ballistic compressor<sup>(1)</sup> to generate transient high pressure gas flows through sample metal nozzles and a combustor test stand<sup>(2)</sup> in which the high pressure products from propellant combustion were similarly used. The period of research covered in this report is from 1 January 1980 to 30 November 1980 during which the present author assumed the direction of the research. Prior to this time Dr. Leonard H. Caveny had directed the program. The change of leadership resulted from Caveny's departure to AFOSR. Work previous to this period was reported to AMMRC by Caveny in August 1980.

The results reported here have all been obtained using nozzles fabricated from 4340 steel, some of which had protective coatings sputtered onto those surfaces exposed to the gas flow. The same starting material was used throughout. Erosive exposure was to high pressure gases generated using the ballistic compressor. No measurements were made using the combustor. Detailed examinations of the samples were made both prior to and post exposure using scanning electron microscopy to obtain topographic and Xray analytical data. Some samples were also studied using scanning Auger techniques. Since the methods of study employed were surface sensitive, the erosion exposures were kept close to those associated with the erosion threshold. In all cases in which erosion occurred the process was associated with a melting and ablation phenomenon. The details of the melting were found to be strongly dependent upon the nature of the gas flow through the nozzle. Attempts were made to control this flow from experiment to experiment but the small nozzle size made accurate control difficult. Variation in the fluid mechanical behavior of the flow between different nozzles is probably the major source of differences in sample to sample erosion for a given gas composition and pressure/time behavior. None of the sample coating procedures employed had a significant effect on the observed erosion. Data from these runs, however, was important in

revealing the role of the fluid flow on the observed erosion and in indicating that the major mass loss occurred at the entrance region rather than uniformly along the nozzle surface.

Some preliminary measurements using a modified thin film gauge have been made and are also reported here. Fabrication problems and gauge failure in the high pressure ambient limited the data obtainable with these devices.

The following sections will amplify topics from the brief summary presented in this introduction.

## II. SAMPLE PREPARATION

All specimens used in this sequence of measurements were prepared from the same 4340 steel billet.<sup>(3)</sup> They had a nominal outside diameter of 14.3 mm and thicknesses ranging from 1.3 mm to 4.8 mm. Nozzle configurations are shown diagrammatically in Figure 1. The "standard" sample thickness was 2.54 mm and the specimen had either a 0.66 mm diameter circular cross section nozzle at its center or a rectangular orifice 2.4 mm wide x 0.18 mm deep located on the center line. For the rectangular orifice samples the specimen was split along a diameter and the nozzle was machined in one half, the fourth side of the nozzle being formed by the planar face of the other semicylindrical section. Some of the circular nozzles were also machined in split samples of standard thickness with the nozzle symmetrically placed in the center of the sample so that each sample section contained half of a nozzle. Whereas the rectangular nozzles had sharp corners, the nozzles of circular cross section were given a shaped entrance so that the uniform nozzle diameter started at approximately 20% of the sample thickness from the entry face. Over this distance the nozzle diameter was changed by about a factor of two in a smooth curve.

Split nozzles of both cross sectional shapes could be examined before and after firing in the ballistic compressor using the SEM or Auger probes. The split configuration also permitted films of various materials to be sputtered onto the nozzle surfaces. For these studies Chromium,  $\text{Al}_2\text{O}_3$  and Boron Nitride films were employed. Films of approximately  $1 \rightarrow 2 \times 10^{-7}$  mm thickness were

deposited on the nozzles, the surfaces of which were cleaned by sputter etching prior to film deposition.

### III. BALLISTIC COMPRESSOR CONDITIONS

Two sample holder configurations were available for the ballistic compressor one of which could take four samples and the other a single sample. Both holders were instrumented with a piezoelectric pressure transducer to measure  $p(t)$  during the erosion exposure. Some preliminary measurements were made using the four sample head, however, considerable scatter in the mass loss occurred between the samples since the fluid mechanics of the flow favored that nozzle which started to erode first. The measurements reported below were, therefore, made using the single sample head.

Gases of the desired composition were introduced into the compressor from a premixing vessel that held enough gas for approximately three firings. The driven gas compartment was evacuated using a mechanical pump prior to the introduction of the test gas. In all cases the driving gas was nitrogen. By adjusting the pressure of the driving gas the peak pressure of the driven gas could be controlled and pressures in the range between  $1.4 \times 10^8$  Pa (20 KPsi) and  $3.8 \times 10^8$  Pa (56 KPsi) were employed. Pulse durations were on the order of 3 msec and measurements made with the thin film temperature transducers indicated that the peak temperature occurred at approximately the same time as the peak pressure. Pressure and temperature data were recorded using a Biomation 1015 waveform recorder and analyzed using the Hewlett Packard computer. Typically, the computer was used to integrate the area under the pressure time curve above some threshold pressure at which the onset of erosion occurred. This pressure threshold was taken to be 60 MPa on the basis of extrapolated mass loss measurements.

For the majority of the runs to be discussed below pure nitrogen or oxygen-nitrogen mixtures were used as the driven gas. Some measurements were made using  $H_2/N_2$  gas mixtures. In all cases the gases used were nominally dry.

#### IV. MASS LOSS EXPERIMENTS

A global measure of the erosive effects of a gas flow of given composition through a nozzle is the mass loss experienced by the sample. As will be discussed further below this is only an approximate measure of erosion, particularly *near the threshold* for erosion, since reattachment of displaced molten material from the front end of the nozzle occurs on the cold surfaces towards the nozzle exit. It is also important to determine if the peak pressure threshold at which erosion starts to occur is the relevant parameter for these studies. In order to gain insight into this question data was obtained using pistons of different mass in the ballistic compressor. Both a 2.68 Kg and a 1.34 Kg piston were employed and peak pressures in the range between  $1.3 \times 10^8$  Pa and  $3.8 \times 10^8$  Pa were achieved by adjusting the driving gas pressure. Figure 2a shows mass loss data for a set of twelve samples, exposed to a 40%  $O_2$ , 60%  $N_2$  dry driven gas, plotted against the peak pressure. The line plotted through the data points is a least squares fit to the points and it can be seen that the fit is poor. In Figure 2b the same erosion data is plotted against the area under the pressure time curve above a pressure of 60 MPa. It is seen that the least squares fit through these points is in much better agreement with the data than for the previous representation.

#### V. SEM STUDIES OF NOZZLES

##### a) Rectangular Nozzles

Due to the ease with which they could be coated with protective films and examined in the scanning electron microscope, a series of measurements were made on nozzles of rectangular cross section in split 4340 samples (Figure 1a). The leading and trailing edges of these samples were sharp as were the longitudinal corners in the nozzle. Runs were made in the ballistic compressor using  $O_2/N_2$  mixtures with an oxygen content of 0%, 2%, 5%, 10% and 15% and a nominal peak pressure of  $3.4 \times 10^8$  Pa. For each of these exposures the integrated area under the pressure time curve above the threshold pressure of 60 MPa was  $15.4 \pm 0.2$  Pa-sec.

As expected for these test conditions, in which the adiabatic compression of a driven inert gas does not raise the surface temperature to the melting point of the steel nozzle under test, no erosion was visible on the sample exposed to dry nitrogen. When oxygen was a constituent of the flow, erosion took place indicating that the reaction between the oxygen and the steel was contributing to an increase in surface temperature and causing local melting. For flows with a low oxygen content the erosion was confined to the entrance of the nozzle. As the oxygen content was increased the eroded region penetrated into the nozzle away from the leading edge. The erosion was not uniform across the transverse dimension of the nozzle and was asymmetric between the two half sections. In that half of the sample into which the nozzle was machined erosion was greater in the corners than on the adjacent planar surfaces. Rounding of the leading edge of the nozzle always occurred and melted material from this region was pushed by the flow back into the nozzle where some resolidification occurred. On the planar face of the semicylindrical segment that formed the fourth, closing side of the nozzle the erosion pattern was greatest towards the nozzle center line and least at the corners where this segment was in contact with the other semi-disc. This asymmetry between the two sections of the nozzle is not understood but is probably associated with the discontinuity in the thermal properties of the nozzle disc produced by the split along its major diameter and the asymmetric placement of the nozzle with respect to this plane.

A series of tests made with this same nozzle configuration involved samples onto which various protective films had been deposited by sputtering. Prior to film deposition the nozzle surfaces were sputter-etched in the argon atmosphere of the turbo-pumped sputtering machine. After surface preparation in this way films between 1000 and 2000Å in thickness were deposited on the surface of the nozzle. During sputtering the nozzle discs were in thermal contact with a water-cooled stage and the deposition of the protective films occurred with the sample at approximately 20°C. Films of Aluminum Oxide, Boron Nitride and Chromium were RF sputtered from targets of these materials in the argon ambient of the machine. Some departure from stoichiometry is expected to have occurred for the insulating oxide and nitride films.

The samples protected with circa 1000Å Aluminum Oxide films were exposed to oxygen-nitrogen driven gas mixtures with nominal compositions of 1%, 2%, 5% and 15% oxygen. The peak pressure of the driven gas was circa  $3 \times 10^8$  Pa for each run. Examination of the nozzles with the SEM and light microscopy prior to the erosion test indicated that the  $Al_2O_3$  film was continuous throughout the length of the nozzle but that the front and rear faces of the sample disc were not protected by the film due to shadowing effects during sputter deposition.

Erosion was found to occur in this series of samples in a manner similar to that observed for the uncoated nozzles. Examination of the SEM topography (Figure 3a) suggests that melting initially occurred at the sharp leading edge of the nozzle on the unprotected front face. Material was removed from this stagnation region by the gas flow and the unsupported film within the nozzle was then broken away permitting further surface melting to occur in the region of flow reattachment. This molten material was also displaced by the gas flow and some of it resolidified on the downstream, and still protected, nozzle surface. Droplet spatter patterns on this protected downstream surface indicated that some molten material was carried completely through the nozzle. It is only this removed material that would be measured in mass loss experiments rather than the total amount of material displaced as a result of melting processes at the nozzle entrance.

S.E.M. examination of a sample exposed to a 1%  $O_2$ , 99%  $N_2$  driven gas flow showed the initial erosion process in more detail and demonstrated the importance of the flow details in the observed behavior (Figure 3b). For this sample leading edge melting was also observed presumably resulting from high heat transfer rates in this stagnation region and poor heat removal from the corner. Immediately behind this leading edge the  $Al_2O_3$  film remained intact in the region where the boundary layer was expected to be thick. In the downstream region where flow reattachment occurred the  $Al_2O_3$  film was removed and surface melting and material displacement was observed. Further towards the exit of the nozzle the  $Al_2O_3$  film was again intact and displaced material re-adhere to the protected surface.

As the oxygen content of the driven gas flow was increased the leading edge melting became more pronounced and the resolidified layer on top of the still undamaged protective film toward the rear of the nozzle also increased in thickness. With the 15% oxygen flow (Figure 3c) the topographic evidence suggested that the resolidified material displaced by the flow did not adhere strongly to the substrate. Film cracking occurred and it is probable that fragments of the solidified film were removed from the nozzle by the gas flow. The details of this process would be expected to give rise to considerable scatter in mass loss measurements made under these flow conditions.

Similar behavior was observed on the samples coated with Boron Nitride and Chromium protective films. Leading edge melting occurred in the flow containing oxygen, the molten material was transported back into the nozzle by the gas flow and resolidification of the displaced material occurred on the downstream surfaces of the nozzles.

The shape of the erosion profile produced by these "threshold" flows on both unprotected and protected 4340 steel surfaces indicates that the details of the fluid flow are important in determining the overall erosion behavior. The erosion profile suggests that the boundary layer behavior may control the erosion in these high speed flows. For these sharp cornered rectangular nozzles, erosion always seems to occur at the corner of the flat face facing the ballistic compressor where flow stagnation is expected to occur. Behind this sharp leading edge a thicker boundary layer will be formed as the flow over the front surface of the sample disc changes direction to exit through the nozzle. In this region the boundary layer would be expected to have its maximum thickness and the SEM topography suggests that the erosion is less in this region. Downstream of this virtual throat the flow reattaches to the walls of the nozzle and the erosion is increased. Downstream of this region where a viscous flow is established displaced material overlays the initial nozzle surface and solidifies, presumably due to heat losses to the body of the nozzle and altered heat transfer from the gas flow.

## b) Circular Nozzles

In an attempt to improve the gas flow conditions through the test nozzles, specimens having a circular cross section and a shaped entrance were prepared. These had either the split configuration of Figure 1b or the solid form of Figure 1c. The small nozzle size needed to permit the desired peak pressures and flow durations to be obtained made it difficult to control the exact form of the nozzle profile and preliminary experiments indicated that surface flaws introduced during the fabrication of the nozzle also influenced the erosion behavior. In order to minimize these effects subsequent nozzle surfaces were polished with diamond lapping compound using a final grit size of 20 microns.

When the changed gas flow conditions are taken into account the erosion behavior of these nozzles is seen to be essentially the same as for the nozzles of rectangular cross section. Some erosion occurred on the entrance profile to the straight section of the nozzle at the higher oxygen concentrations (10%, 15%). The main erosive activity, however, occurred in the entrance to the straight section and downstream of this region (Figure 4). Melting had clearly taken place and the melted material had been displaced by the gas flow. Some of the material displaced by the flow reattached to the downstream surfaces of the nozzles and reattachment patterns indicated that material was also blown out of the nozzles. As in the case of the rectangular nozzles, cracks occurred in this resolidified overlayer. Gas leakage between the nozzle halves towards the nozzle exit caused erosion to extend from the nozzle onto the abutting flat faces of these two sections.

## VI. AUGER MEASUREMENTS ON THE NOZZLES

The absence of erosion under the test conditions when the driven gas was pure nitrogen and the observed melting and ablation for oxygen-nitrogen gas mixtures clearly indicates that chemical attack of the nozzle surfaces is important in taking the surface temperature of the samples above their melting point. Under typical test conditions the maximum nozzle surface temperature reached with an adiabatically compressed inert driven gas would be on the order of 1600 K and the reaction with the gas flow would therefore need to increase the surface temperature<sup>(4)</sup> by circa 200 K in order for melting to occur.

In order to examine the chemical composition of the displaced material to see if evidence of a chemical interaction could be found, Auger measurements were made on nozzles that had been exposed to flows containing 0%, 5% and 10% oxygen. Both spot elemental analysis and scanning Auger photography employing Auger electrons characteristic of a given element were made at various locations in the nozzles which were of rectangular cross section. Since the samples had been exposed to the atmosphere after being taken from the ballistic compressor and before being placed in the Auger apparatus, the specimen surfaces were bombarded with 1 KeV argon ions for 7.5 mins prior to the scanning Auger photographs being made. Spot analysis of the flat nozzle surface that was unexposed to the gas flow made before and after this ion bombardment indicated that surface contamination by oxygen, nitrogen and carbon was reduced by this treatment. A small Auger peak due to implanted argon was visible in the post bombardment spectrum (Figure 5a) with the major constituents being Fe and C. Figure 5b shows the corresponding Auger specimen for the molten material displaced by the erosion process that had resolidified in the nozzle. It is seen that, even after the ion bombardment to remove surface contaminants, this spectrum had a strong line associated with oxygen in addition to the lines of carbon and iron.

In order to clarify the spatial distribution of elements in the nozzle, scanning Auger photographs were made at a magnification of 300x using the Auger electrons associated with Fe (694 eV) and Oxygen (510 eV) together with a secondary electron scanning microscope image of the same sample area. As seen in the SEM image of Figure 6a the boundary between the displaced material and the uneroded surface runs approximately across the center of the field of view. The iron and oxygen images shown in Figure 6b and 6c respectively indicate that the uneroded surface has a high iron content and a low oxygen content, a fact consistent with the spectra shown in Figure 5, and that the melted and resolidified material that was displaced by the flow has a high oxygen content and a low iron content. This data strongly supports the contention that an oxidative reaction with the iron surface of the nozzle is needed to raise its temperature above the melting point and permit ablation to occur.

## VII. DISCUSSION OF THE EROSION DATA

All of the data presented above indicates that when erosion of 4340 steel nozzles occurs upon transient exposure to high pressure oxygen-nitrogen mixtures, material removal is due to melting and the partial ablation of the molten material by the gas flow. The fact that this process does not occur under these same threshold conditions for a dry nitrogen flow suggests that an oxidation reaction is required to raise the surface temperature of the nozzle above the melting point of the 4340 steel. The mass loss data presented in Figure 2 shows that the mass loss scales linearly with the integrated area under the pressure-time curve above a threshold pressure. For the measurements shown the threshold pressure was circa 60 MPa.

The scanning electron micrographs made of the erosion features in both rectangular and cylindrical nozzles under near threshold conditions for erosion clearly show that resolidification of displaced molten material occurs towards the exit of the nozzles. This observation indicates that care should be taken in interpreting mass loss measurements since these only measure the amount of material removed from the nozzle rather than the total amount of material melted and displaced by the flow. This observation may account for the observed scatter in mass loss measurements made under essentially similar compressor conditions especially at the higher oxygen contents where cracking of the resolidified overlayer occurs and solid fragments may also be removed by the flow.

Comparison between the rectangular and circular nozzles indicates that the details of the fluid mechanics of the flow are important in the erosion process. Erosion is high in regions associated with stagnation and flow reattachment and lower in regions where the boundary layer would be expected to be thick or the flow to be viscous. The small size of the nozzles necessitated by the performance of the ballistic compressor makes it hard to achieve exactly repeatable nozzle configurations and data obtained with this equipment is therefore sensitive to slight differences between the samples.

Protective overlayers of  $Al_2O_3$ , Boron Nitride and Chromium were found to have little effect on the near threshold erosion behavior. Film failure occurred

at the entrance to the nozzles and at the point at which flow reattachment took place. These measurements were of value, however, in clearly indicating that some molten material displaced by the flow resolidified towards the exit of the nozzles and that dimension changes in this region were due to this process rather than to oxide growth as suggested by Alkidas et al.<sup>(5)</sup>

It is also of interest to note that many of the nozzle surface features observed in the present measurements are similar to those found by Vassallo and Brown.<sup>(6)</sup> These authors had the advantage of a system capable of making measurements on sample nozzles of circa 20 mm diameter, a size which permitted much better control of nozzle contours and gas flows.

VIII. THIN FILM GAUGES

In an attempt to obtain a measured value of the adiabatic gas temperature in the ballistic compressor as a function of time and to experimentally measure the energy released by a 4340 film during an oxidizing reaction in the ballistic compressor a thin film platinum resistance gauge configuration was explored. The structure of the active elements of these gauges is shown in Figure 7a. A platinum film having a resistance in the range between 100 and 200 ohms was deposited on a pyrex disc using an airbrush technique and Hanovia liquid bright platinum 05-x. This compound was decomposed to leave a platinum film on the pyrex by firing at 720°C in an air ambient. Contact to the thin film platinum resistor was made with copper leads brought through slots in the edge of the disc using a silver loaded conductive epoxy to provide good electrical continuity. For the purpose of making comparisons between various gauge configurations some thin films were used without further processing other than mounting in a steel holder that could be introduced into one of the nozzle slots of the 4 sample head of the ballistic compressor. Other samples were given an additional protective coat of Boron nitride using the sputtering apparatus to produce a film of circa  $1 \times 10^{-6}$  m thickness. Some of these samples were then mounted in the steel holder for the compressor while one sample had an additional  $1 \times 10^{-6}$  layer of 4340 steel sputtered onto its surface, overcoating the central region of the platinum resistance and nitride film. This sample was also mounted in a steel holder for the ballistic compressor.

In tests of these thin film gauges, up to three could be mounted in the compressor as shown diagrammatically in Figure 7b. A nozzle was put into the fourth aperture of this head to provide the desired pressure time transient during the compressor firing. Both pure nitrogen and oxygen nitrogen driven gas mixtures were employed in these tests. The gauges were connected to constant current sources and about 1.0 mA was passed through the gauge circuit. In a typical firing of the ballistic compressor this would give a peak output voltage of 100 mV, the complete voltage transient being recorded by the Bio-mation 1015 waveform recorder together with the output of the pressure transducer.

The temperature coefficient of resistance of the gauges was determined by making resistance measurements with the gauge in a constant temperature oven. Calibration was taken up to 100°C and the data fit with a linear regression procedure to the relationship:

$$R(T) = R_0(1+AT)$$

where the temperature T is in degrees centigrade. A best fit to the data indicated that the constant A had a value of circa  $2 \times 10^{-3}$ .

Four test firings were made to compare the bare platinum gauge to the gauge with an overcoating of boron nitride and 4340 thin film. A peak pressure of circa  $2 \times 10^8$  Pa (30 KPSI) was used in these measurements and both pure Nitrogen and 5% and 10%  $O_2/N_2$  mixtures were used. For each firing the maximum temperature rise indicated by the coated platinum gauge was approximately half that indicated by the uncoated gauge. The peak temperature indicated by the uncoated platinum gauge in the pure nitrogen runs was only 650K compared to an expected gas temperature of circa 2400K. As indicated above the temperature-time behavior showed a peak at approximately the same time in the pressure cycle as the pressure itself but had a slower decay to its prefiring value. After 4 tests the gauges produced had failed electrically and the measurements were discontinued.

References

1. A. C. Alkidas, E. G. Plett and M. Summerfield, AIAA Journal 14 (1976) 1752.
2. A. Gany, L. H. Caveny, M. Summerfield and J. W. Johnson, Proceedings of 1978 JANNAF Propulsion Meeting, February 1978.
3. Republic Steel Corporation, Heat #8043738, 0.395C, 0.74Mn, 0.008P, 0.007S, 0.27Si, 0.75Cr, 1.72Ni, 0.22Mo.
4. DAAPER code developed at the Guggenheim Laboratory, Princeton University, (1979).
5. A. C. Alkidas, S. O. Morris, C. W. Christoe, L. H. Caveny and M. Summerfield, AMMRC, CTR-77-25, Final Report on contract #DAAG46-75-C-0088.
6. F. A. Vassallo and W. R. Brown, ARBRL-CR-00406. Final report on contract #DAAK11-77-C-0018.

Figure Captions

Figure 1. Dimensions of 4340 steel nozzles used in the present measurements.

Figure 2. Mass loss data for 4340 steel nozzles exposed to a 40% O<sub>2</sub>, 60% N<sub>2</sub> dry gas mixture.

- a) Data plotted as a function of peak pressure.
  - b) Data plotted as a function of area under the pressure-time curve.
- Lines shown are least squares fits to the data points.

Figure 3. a) Secondary electron image of an eroded nozzle that had an Al<sub>2</sub>O<sub>3</sub> film sputtered onto its surface prior to the erosion exposure 2% O<sub>2</sub>, 98% N<sub>2</sub> dry gas mixture. Magnification 100x.

b) Secondary electron image of an eroded nozzle protected by a sputtered Al<sub>2</sub>O<sub>3</sub> film. 1% O<sub>2</sub>, 99% N<sub>2</sub> dry gas mixture. Magnification 300x.

c) Secondary electron image of an eroded nozzle protected by a sputtered Al<sub>2</sub>O<sub>3</sub> film. 15% O<sub>2</sub>, 85% N<sub>2</sub> dry gas mixture. Magnification 50x.

Figure 4. Secondary electron image of entrance to a split circular nozzle exposed to a 10% O<sub>2</sub>, 90% N<sub>2</sub> dry gas mixture. Magnification 100x.

Figure 5. a) Auger analysis of 4340 nozzle surface that was unexposed to erosive flow following bombardment with Argon ions to remove surface contaminants.

b) Auger analysis of displaced molten material from the same nozzle also following Argon ion bombardment. Erosive exposure was to 5% O<sub>2</sub>, 95% N<sub>2</sub> dry gas mixture.

Figure 6. a) Secondary electron image of a nozzle in the scanning Auger apparatus showing the boundary between resolidified flow and the initial nozzle surface. 5% O<sub>2</sub>, 95% N<sub>2</sub> dry gas mixture. Magnification 300x.

b) Scanning Auger image of the same region using the Iron 648 eV peak. Bright areas indicate a large iron signal.

Figure 6. c) Scanning Auger image using the oxygen 510 eV peak. Note that the resolidified flow has a high oxygen content whereas the initial nozzle surface gives a low oxygen signal.

Figure 7. a) Diagram of the active elements of the thin film Platinum Resistance Gauges.

b) Nozzle and gauge configuration used for the ballistic compressor tests.

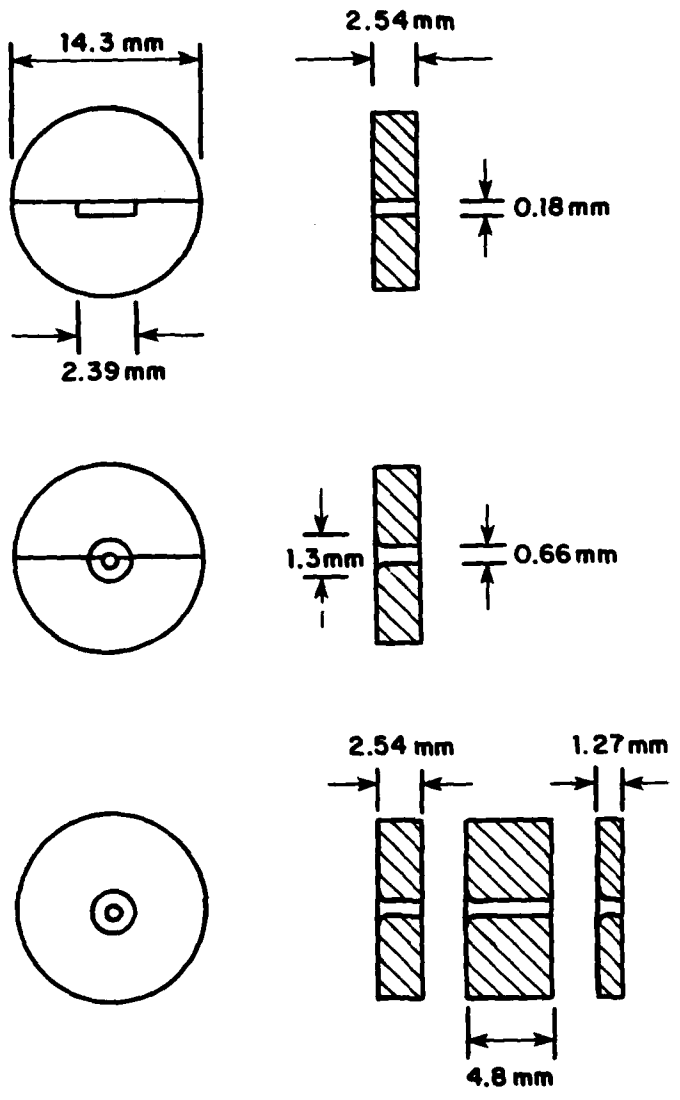


Figure 1

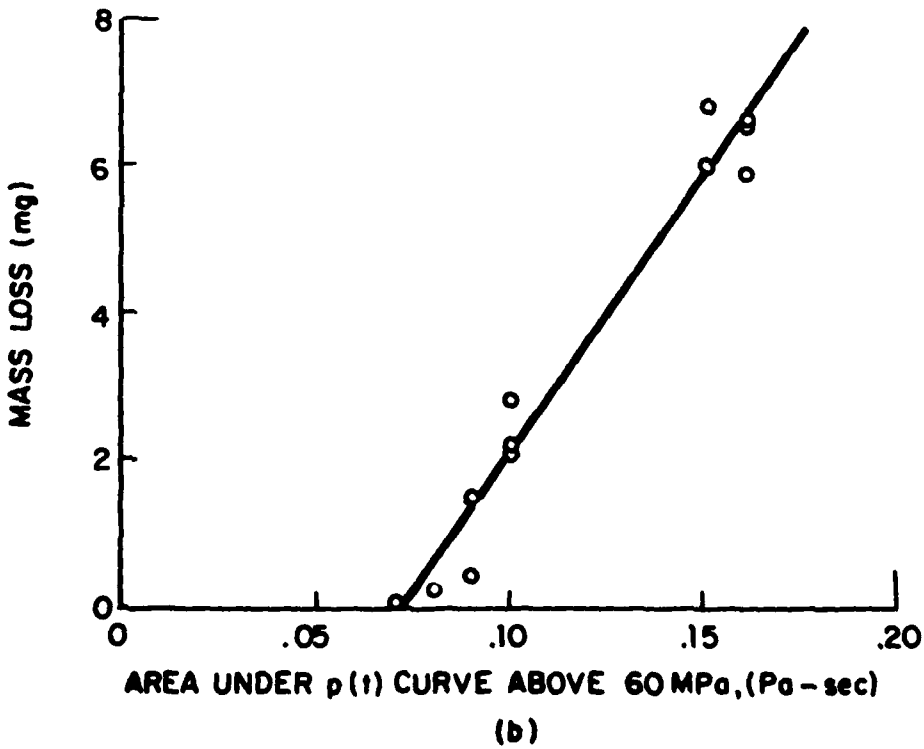
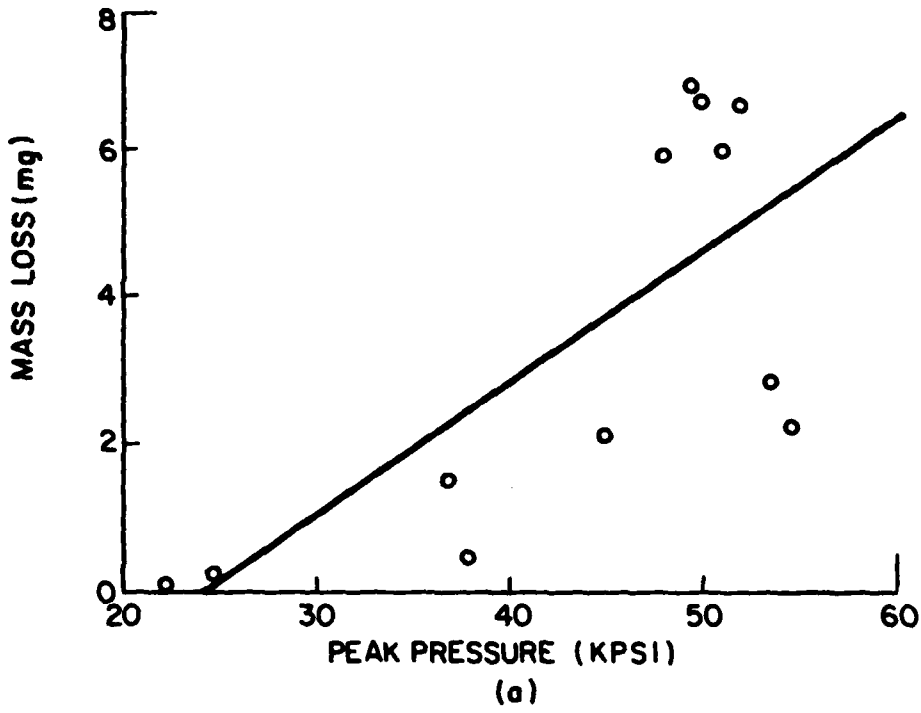
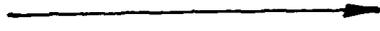
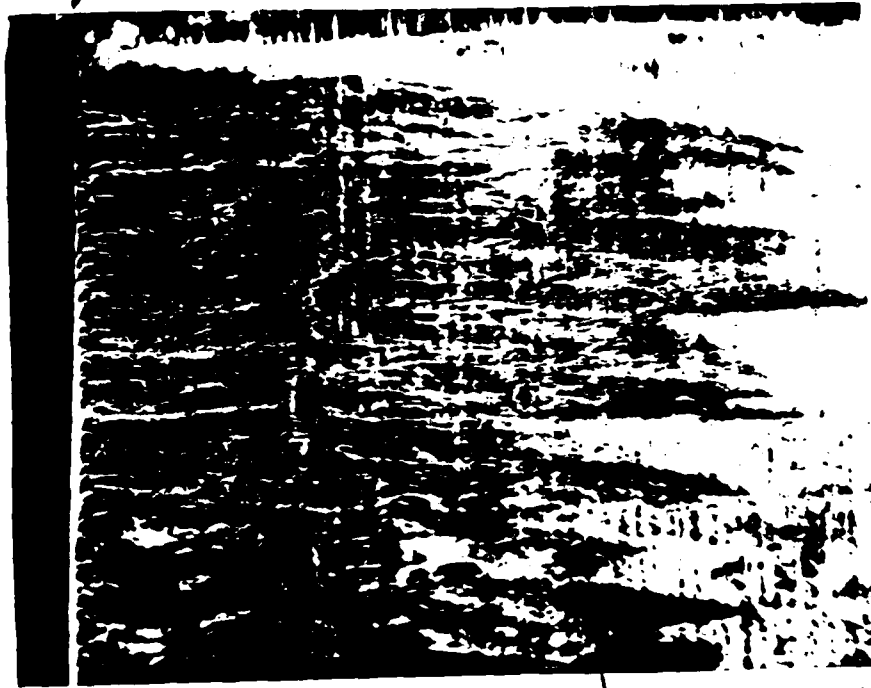


Figure 2

FLOW DIRECTION



Leading Edge of nozzle



Eroded Surface

Surface still  
protected by  
 $Al_2O_3$  layer

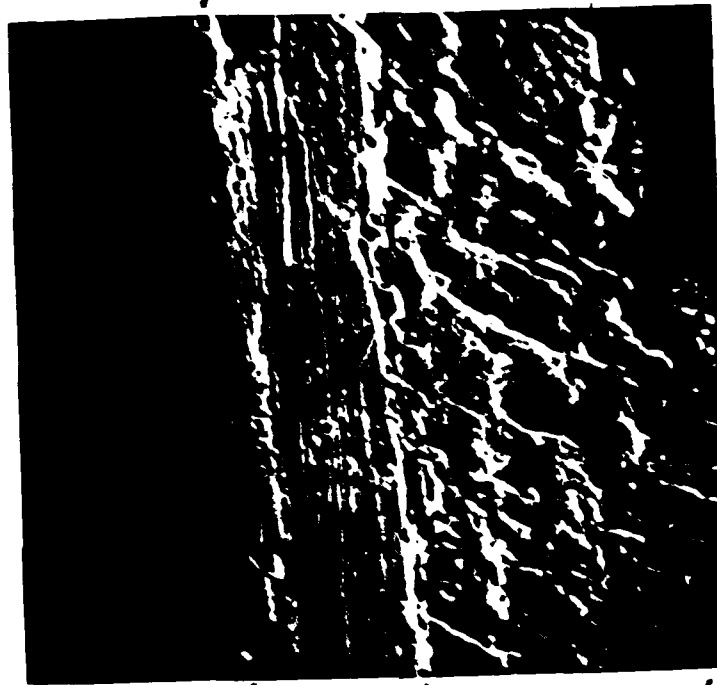
Magnification  
100x

Molten material that has been  
displaced by the gas flow and  
resolidified on the  $Al_2O_3$   
protected surface

Figure 3a

FLOW DIRECTION

Leading Edge of Nozzle



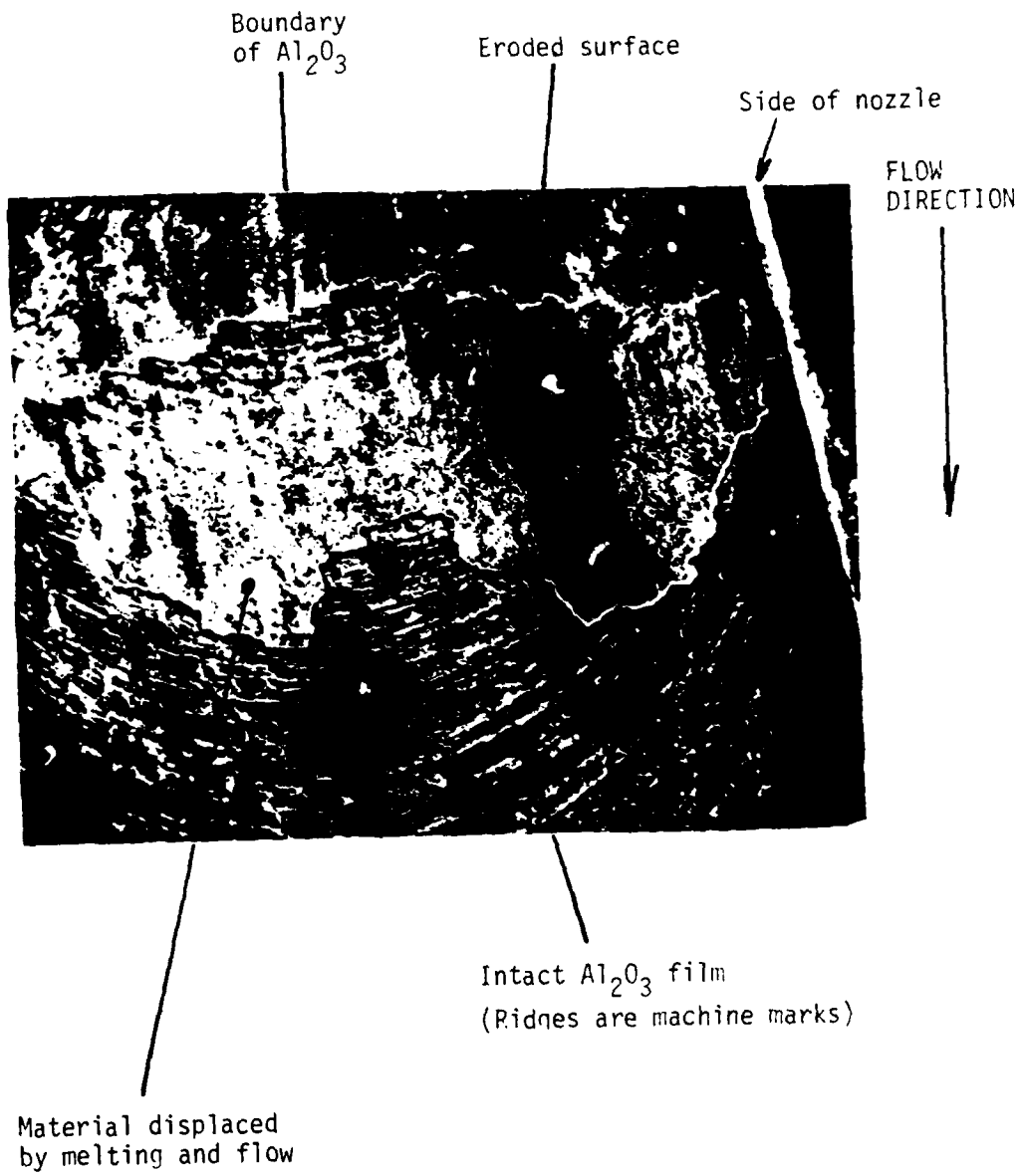
Melting rounds leading edge

Film removal, melting and flow in reattachment zone

Al<sub>2</sub>O<sub>3</sub> film still protecting surface in the region of the thick boundary layer

Magnification 300x

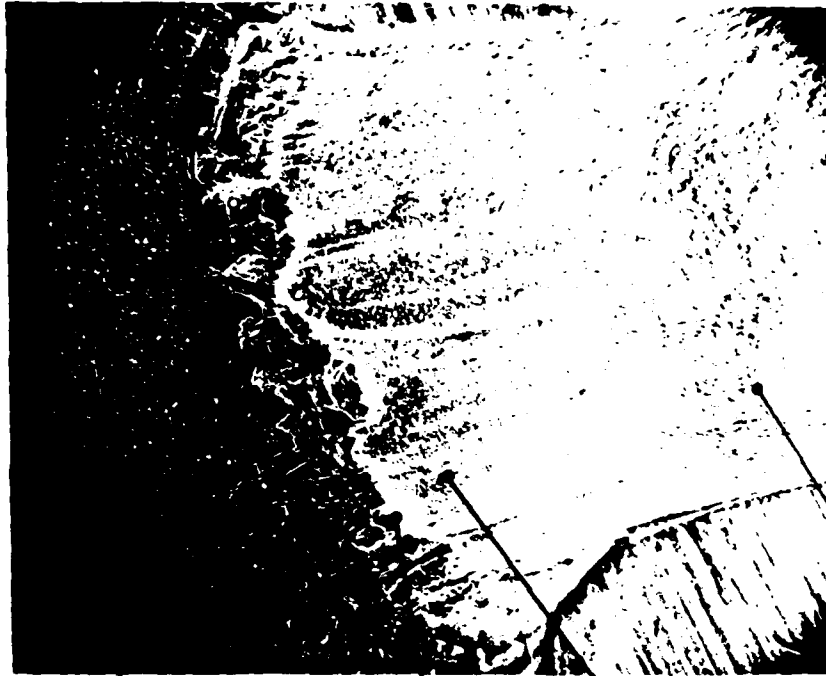
Figure 3b



Magnification 50x

Figure 3c

FLOW DIRECTION



Entrance profile  
of nozzle

Boundary of major  
erosion

Extensive  
material removal

Flowed  
material

Magnification 100x

Figure 4

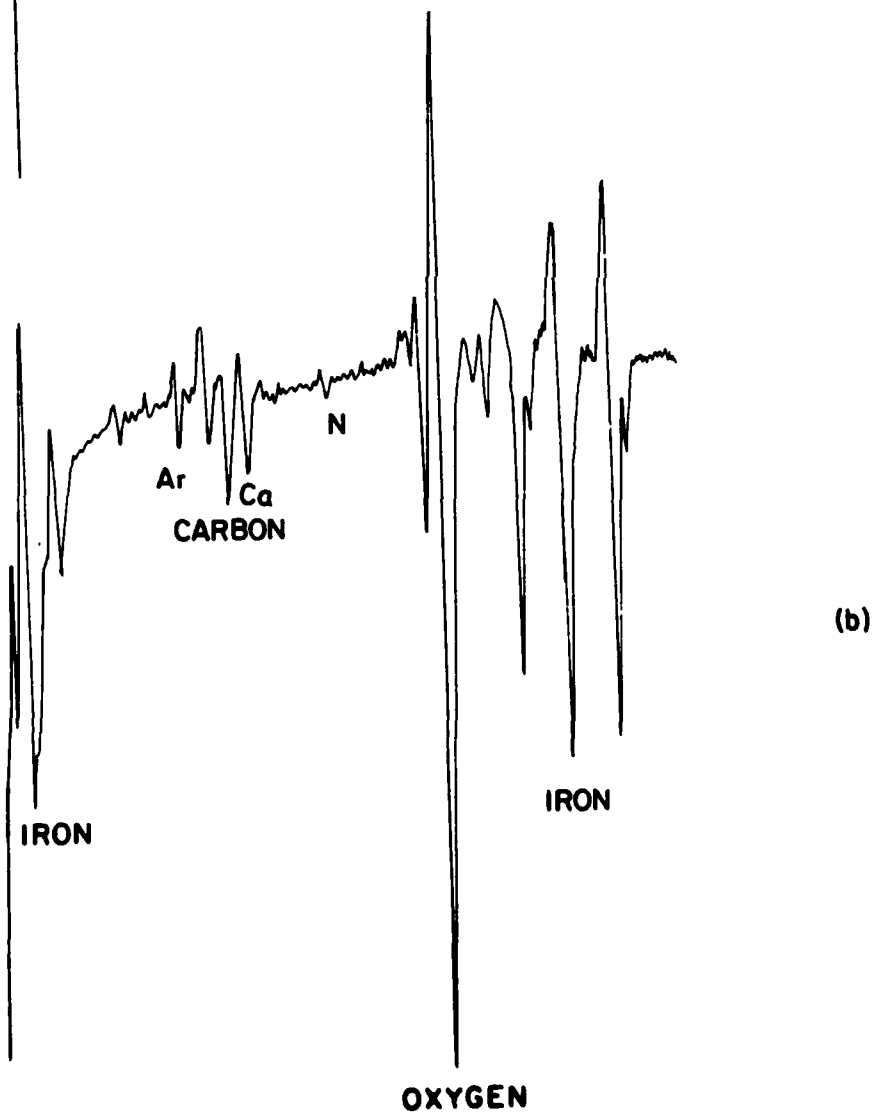
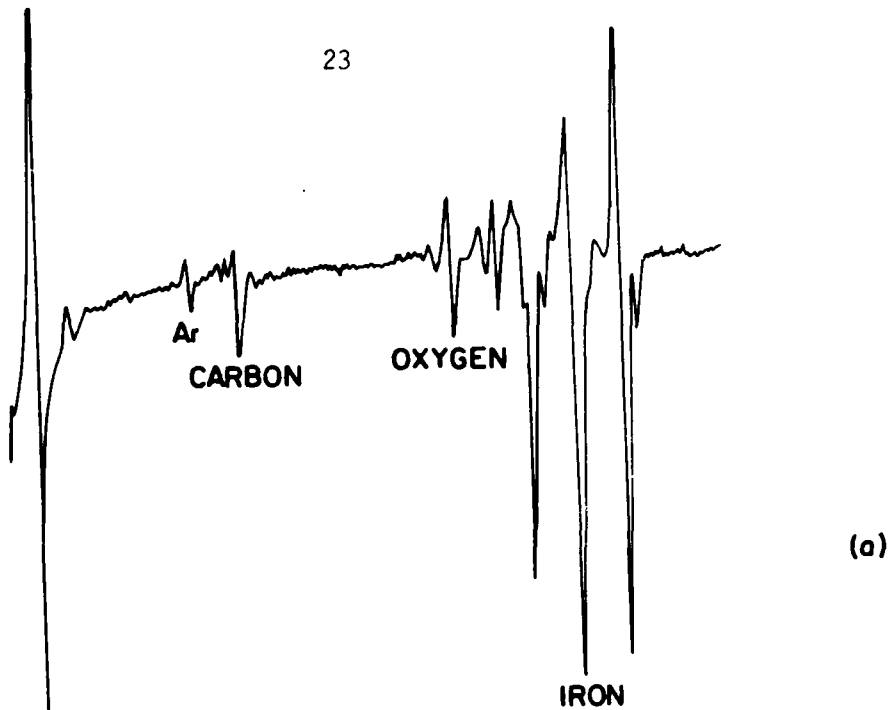


Figure 5

FLOW  
DIRECTION



(a)



Resolidified flow

Initial nozzle surface



(b)

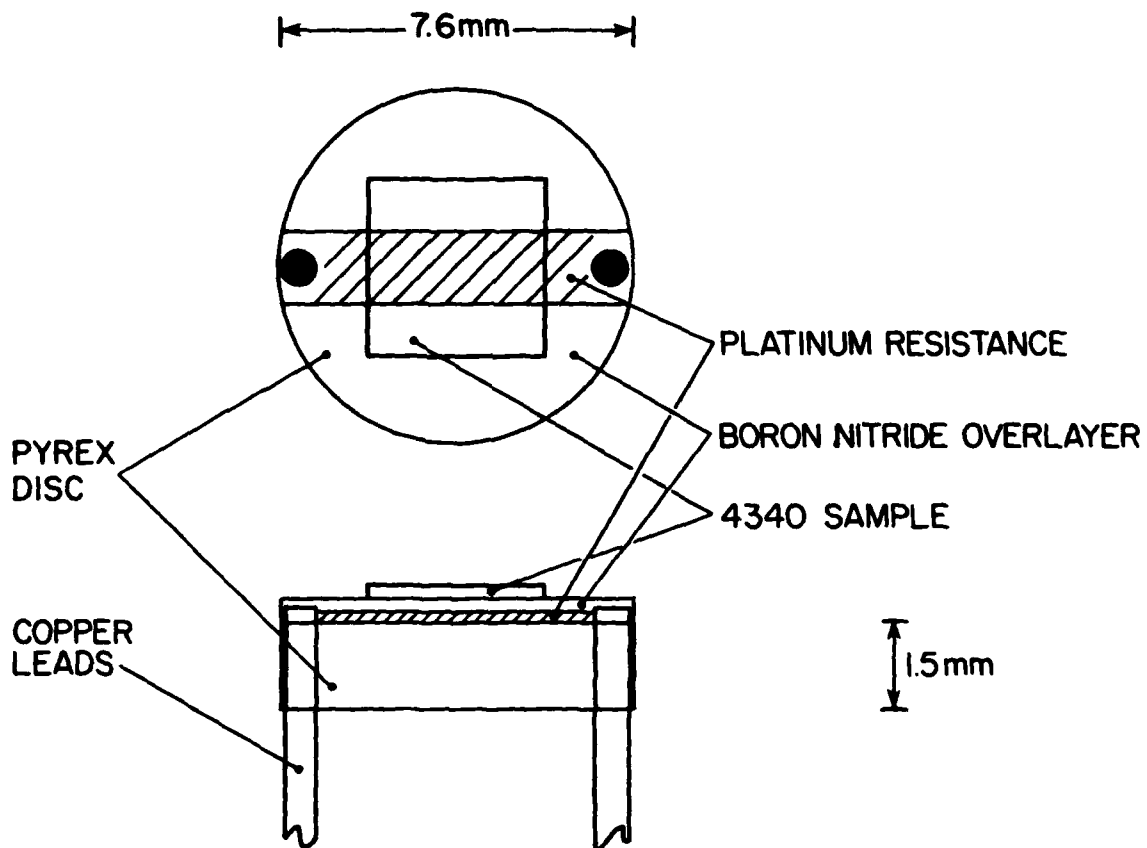
Resolidified flow

Initial nozzle surface

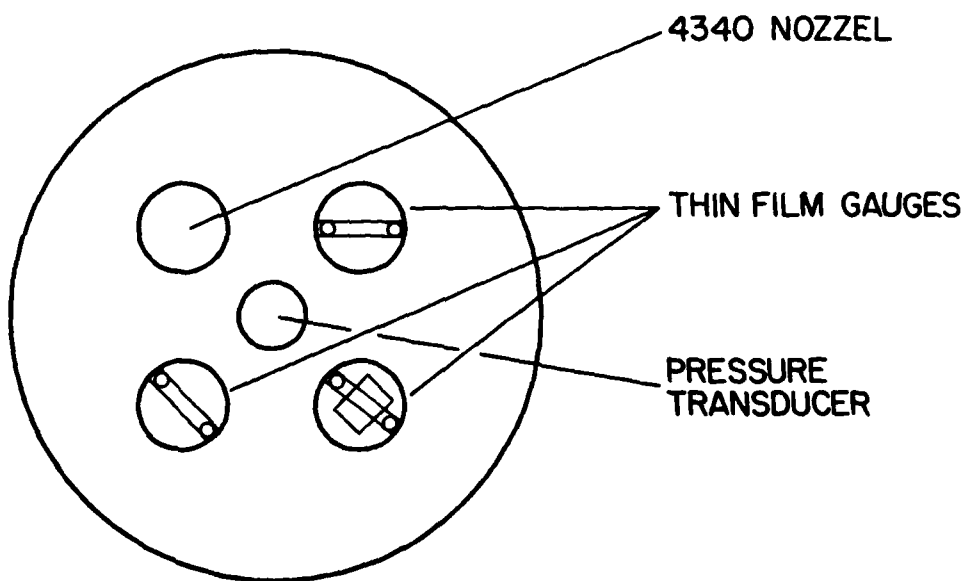


(c)

Figure 6



(a)



(b)

Figure 7